Effects of Variable and Anisotropic Diffusivities in a Steady-State Diffusion Model

LAURENCE ARMI

Scripps Institution of Oceanography, La Jolla, CA 92093

DALE B. HAIDVOGEL

Woods Hole Oceanographic Institution, Woods Hole, MA 02543

(Manuscript received 22 February 1982, in final form 27 April 1982)

ABSTRACT

The hypothesis that variations in eddy diffusivity may account for some aspects of the observed distributions of oceanic scalars is examined by generating solutions to the diffusion equation with spatially variable and/or anisotropic eddy diffusivity. In particular, the solutions generated here demonstrate how a purely diffusive field, with variable and anisotropic diffusion, can itself generate tongue-like property distributions. Although tongues of various oceanic properties have often been interpreted as due primarily to advective effects, such interpretations must be viewed with caution when the gradients of eddy diffusivity are comparable to, or greater than, the local velocity field.

1. Introduction

The hypothesis that variations in eddy diffusivity may account for some aspects of the observed distributions of oceanic scalars was suggested in an earlier paper (Armi, 1979). Further study, primarily with a numerical model, is the subject here.

Motivation for this study comes from the growing observational evidence for large and fairly rapid spatial variability of the eddy energy field of the oceans (cf. Fuglister, 1954; Wyrtki *et al.*, 1976; Dantzler, 1977; Schmitz, 1977); similar variations are also seen in eddy resolving numerical simulations (Holland, 1978; Schmitz and Holland, 1982). Although as yet only very qualitative prescriptions exist for relating the isopycnal diffusivity field to the eddy energy field (cf. Price, 1981), there are striking similarities between property distribution maps and eddy field maps as can be seen in Figs. 1 and 2 [see also Armi (1979) Figs. 5, 6]. One of our goals here has been to generate solutions to the diffusion equation with a variable diffusion coefficient in an attempt to model the salinity distribution shown in Fig. 1 with a diffusivity field similar to that shown in Fig. 2.

An additional complication studied here is the effect of anisotropy in the diffusivity field. This is suggested by the dynamical constraint due to the variation of planetary vorticity in the north-south direction and no such constraint in the east-west direction. Freeland *et al.* (1975) also present observational evidence from the dispersion of SOFAR floats for a small anisotropy of the horizontal diffusivity.

The result of this study is primarily a catalog of solutions to the steady diffusion equation showing the effects of particularly simple distributions of diffusivities and anisotropy. These solutions illustrate quantitatively as well as qualitatively the simple effects of each. Although the classical interpretation of tongues of various properties, for example, the Mediterranean tongue of the North Atlantic, has been as an advective-diffusive attribute (cf. Needler and Heath, 1975; Richardson and Mooney, 1975), the catalog of purely diffusive solutions shown here suggests that any interpretation of tongue-like property distributions need be put forth with caution when little is known about the degree of anisotropy or variability of the supposed Fickian diffusivity field.

2. The diffusion equation with nonhomogeneous anisotropic diffusion

The two-dimensional steady advective-diffusive equation for a nonhomogeneous anisotropic medium can be written as

$$\bar{u}\cdot\nabla C - \nabla\cdot(K\nabla C) = 0. \tag{1}$$

The tracer concentration C is affected by a velocity field $\bar{u}$ and a diffusivity assumed to have the form

$$K = \begin{pmatrix} K_x & 0 \\ 0 & K_y \end{pmatrix}, \tag{2}$$

where the subscripts x and y represent principal directions. For horizontal isopycnal distributions, these principal directions are east and north, respectively,

0022-3670/82/080785-10$06.50

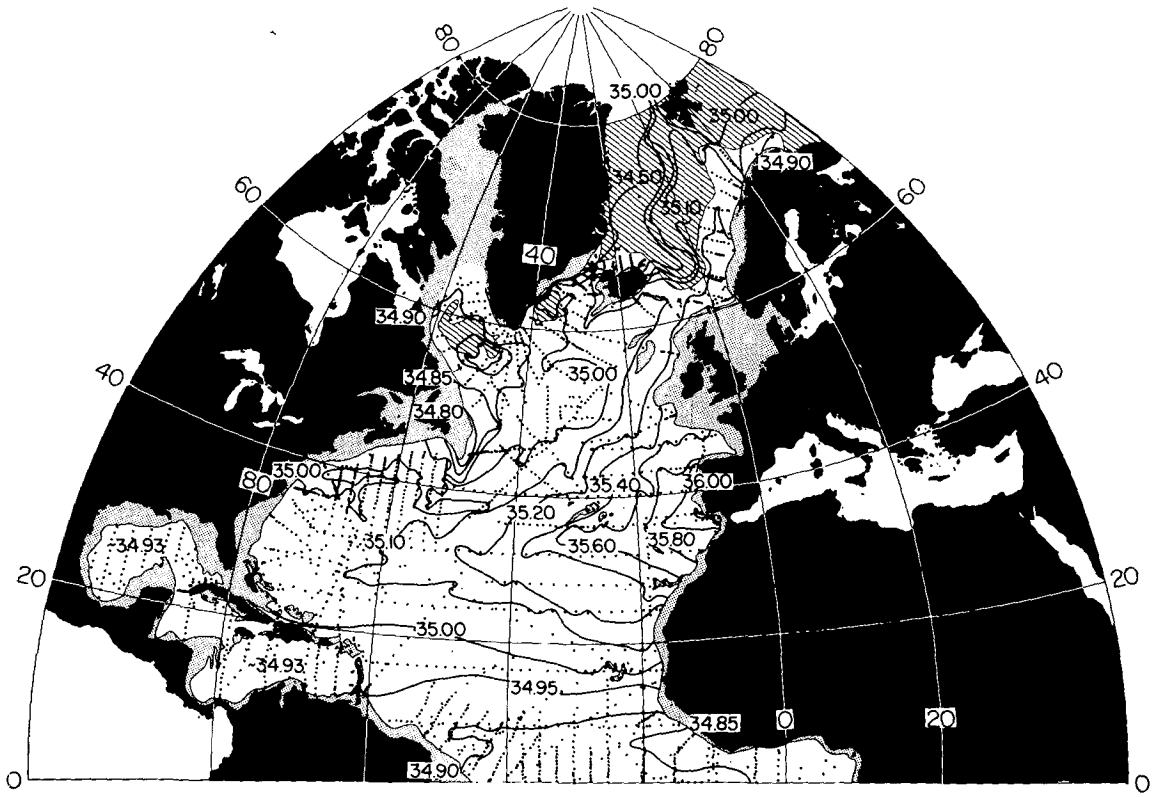

FIG. 1. Salinity (‰) on the density surface chosen to represent Mediterranean outflow water, from Reid (1979). The approximate average depth of this surface is 1 km.

along isopycnals. This form of the diffusivity tensor is also the case of a non-crystalline anisotropic material or orthotropic solid described by Carslaw and Jaeger (1959, p. 41).

With the diffusivity term (2) expanded, the advection-diffusion equation can be written as

$$\left(u - \frac{\partial K_x}{\partial x}\right)\frac{\partial C}{\partial x} + \left(v - \frac{\partial K_y}{\partial y}\right)\frac{\partial C}{\partial y} - K_x\frac{\partial^2 C}{\partial x^2} - K_y\frac{\partial^2 C}{\partial y^2} = 0. \quad (3)$$

Eq. (3) illustrates how variations of the diffusivity act much like an additional advective field in the direction from high to low eddy diffusivity.

Problems of interest here will be those for which the role of advection by the velocity field is weak, particularly in comparison to the advective-like variation in eddy diffusivity, i.e., $u < \partial K_x/\partial x$ and $v < \partial K_y/\partial y$. For the cases treated it will also be assumed that the anisotropy of the diffusivity tensor remains constant, i.e.,

$$\frac{K_x(x, y)}{K_y(x, y)} = A. \quad (4)$$

The effects of anisotropy are then equivalent to a stretching in one direction of the coordinate space (cf. Carslaw and Jaeger, 1959, p. 42). Letting

$$x = A^{1/2}x' \quad (5)$$

and assuming advection to be weak yields the diffusion equation

$$\frac{\partial K_y}{K_y\partial x'}\frac{\partial C}{\partial x'} + \frac{\partial K_y}{K_y\partial y}\frac{\partial C}{\partial y} + \frac{\partial^2 C}{\partial x'^2} + \frac{\partial^2 C}{\partial y^2} = 0, \quad (6)$$

in which the anisotropic effects have been absorbed in the stretched coordinate x'.

If the variation of the diffusivity is assumed to be in only one direction, and this variation is assumed to have the form

$$\frac{dK_y}{K_y dy} = \alpha, \quad (7)$$

then Eq. (6) becomes

$$\alpha\frac{\partial C}{\partial y} + \frac{\partial^2 C}{\partial x'^2} + \frac{\partial^2 C}{\partial y^2} = 0. \quad (8)$$

When α is a constant, Eq. 8 is also the equation for diffusion in the presence of uniform advection for which analytical solutions exist (cf. Carslaw and Jaeger, 1959, p. 266). For the rectangle with north-

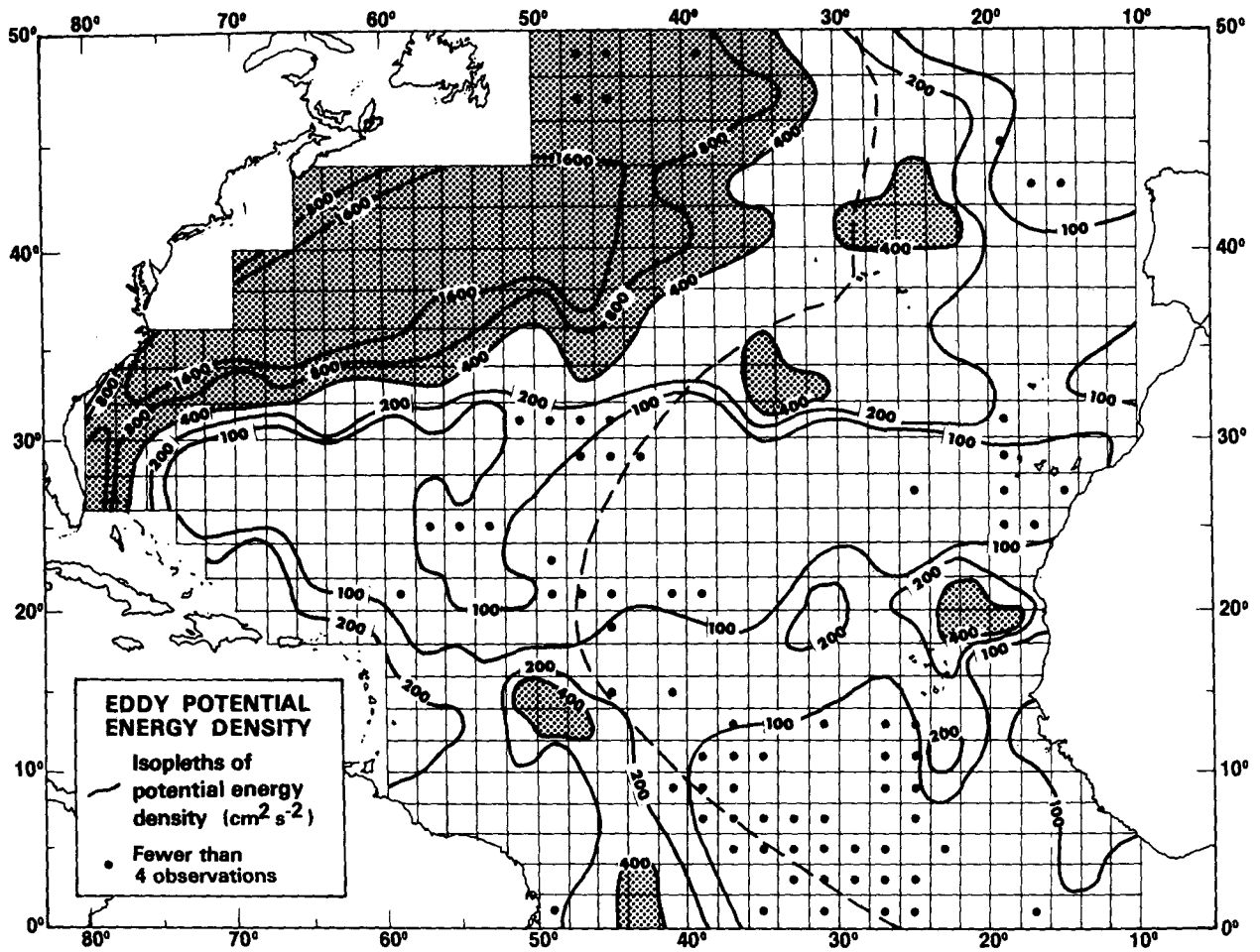

FIG. 2. Estimated potential energy per unit mass arising from mean-squared displacements in the thermocline, from Dantzler (1977).

south length scale L and boundary conditions $C = 0$ at $y = 0, L$, the analytical solution has the form

$$C = e^{\alpha y/2}\phi(x, y), \tag{9a}$$

$$\phi(x, y) = \sin[(n\pi y/L)g_n], \tag{9b}$$

$$g_n = A_n \sinh(q_n x) - B_n \cosh(q_n x), \tag{9c}$$

$$q_n^2 = \left(\frac{n^2\pi^2}{L^2} + \frac{\alpha^2}{4}\right), \tag{9d}$$

where A_n, B_n are constants which must be chosen to satisfy boundary conditions on the remaining north-south boundaries. Inspection of (9d) shows the effects of variable diffusion will dominate the x distribution when

$$\frac{\alpha}{2} > \frac{\pi}{L} \tag{10a}$$

and from (9a), the y distribution when

$$\frac{\alpha}{2} > \frac{1}{L}. \tag{10b}$$

A Peclet number can be formed using the "gradient eddy diffusivity velocity" dK_y/dy. In terms of this Peclet number, the effects of variable diffusivity become important for x and y distribution when

$$\mathrm{Pe} = \frac{dK_y}{K_y dy} L > 2\pi \text{ or } 2, \text{ respectively.} \tag{11a,b}$$

For nonconstant values of α [Eq. (7)], if we define an average Peclet number as

$$\overline{\mathrm{Pe}} = \int_0^L \left(\frac{dK}{K dy}\right) dy, \tag{12}$$

integration of (12) gives

$$\overline{\mathrm{Pe}} = \ln\left[\frac{K(L)}{K(0)}\right]. \tag{13}$$

Hence the effect of variable diffusivity is logarithmic with the ratio of diffusivities.

For oceanic applications, we may expect a north-south ratio of diffusivities in the range of 10 to perhaps 100 based on eddy kinetic energy level maps. This range gives average diffusivity Peclet numbers

between 2.3 and 4.6. From Eq. (11), we may anticipate an effect on north–south property distributions and little effect on east–west distributions for a purely north–south variability of the diffusivity field.

3. Model equation, boundary conditions and solution technique

To investigate directly the potential effects of simple inhomogeneous and/or anisotropic diffusivities on steady-state property distributions, we have examined solutions to the model equation

$$A\frac{\partial^2 C}{\partial x^2}+\frac{\partial^2 C}{\partial y^2}+\left(\frac{A}{K_y}\frac{\partial K_y}{\partial x}\right)\frac{\partial C}{\partial x}+\left(\frac{1}{K_y}\frac{\partial K_y}{\partial y}\right)\frac{\partial C}{\partial y}=0 \quad (14)$$

on the rectangular region $0 \leqslant x \leqslant 1$ and $-0.5 \leqslant y \leqslant 0.5$, where the anisotropy A, here assumed constant, is defined by (4). The model problem [Eq. (14)] is closed by one of two sets of boundary condition assumptions:

either

$$\left.\begin{aligned} C &= 0 && x = 0 \\ & && y = \pm 0.5 \\ \frac{\partial C}{\partial x} &= 10\delta(y_0) && x = 1 \end{aligned}\right\}, \quad (15)$$

or

$$\left.\begin{aligned} C &= 0 && y = \pm 0.5 \\ \frac{\partial C}{\partial x} &= 10\delta(y_0) && x = 1 \\ \frac{\partial C}{\partial x} &= 0 && x = 0 \end{aligned}\right\}, \quad (16)$$

where the delta function (source term) $\delta(y_0)$ is equal to 1 at the "injection point" y_0, and zero elsewhere. Both sets of boundary conditions prescribe absorbing boundaries ($C = 0$) at the northern and southern walls, and a property source ($\partial C/\partial x = 10$) along the eastern wall at some y_0. The western wall is treated either as a property sink [$C = 0$, (15)], or as insulating boundary [$\partial C/\partial x = 0$, (16)]. The actual effective boundary constraints on steady-state property distributions in the ocean are, of course, expected to be much more complicated than those posed here. However, boundary conditions (15) and (16) are easily understood in physical terms, and straightforwardly implemented numerically. A comparison of the effects of the two alternate western boundary prescriptions provides some indication of the range of solutions attainable with (14) and, therefore, the sensitivity to the diffusive character of the bounding surfaces (see below).

Model equation (14), with boundary conditions (15) or (16), has been solved for a variety of inhomogeneous diffusivities $K_y(x, y)$ and anisotropies A on the CRAY 1 system at the National Center for Atmospheric Research (NCAR). The solutions were obtained to fourth-order accuracy on a 65×65 finite-difference grid using the NCAR elliptic equation solving package LIPTIC. [Briefly, an initial second-order solution is determined on the finite-difference grid by an efficient LU decomposition of the resulting sparse (block tridiagonal) matrix equation. A fourth-order solution is found thereafter by the method of deferred corrections—see, for instance, Haidvogel and Zang (1979).] A variety of analytic test problems were performed to evaluate the accuracy of the numerical solutions thus obtained. These analytic tests gave very small relative errors (10^{-6} or less).

4. Discussion of results

The catalog of solutions, generated to investigate potential effects of simple anisotropic and/or inhomogeneous diffusivities on steady-state property distributions, is discussed below. We first look at the effects of anisotropy in a constant diffusivity field.

The effects of varying the degree of anisotropy of the diffusion field are shown in Fig. 3. The diffusivity is kept constant ($K_y = 1$) and only the anisotropy was varied. Both the upper and lower frames of Fig. 3 show solutions for absorbing boundaries at the northern and southern walls and a property source in the center of the eastern wall. The western wall is treated in one of two ways: in the upper frames as an insulating boundary, in the lower frames as a sink. A complete description of the boundary conditions can be found in the previous section. The effects of anisotropy are equivalent to a stretching in one direction of the coordinate space [Eq. (5)]. For anisotropies of 5 and 10, clear tongue-like property distributions are seen; in the neighborhood of the source, the aspect ratio of the tongue is given by $A^{1/2}$ [Eqs. (5), (6)]. The tongue-like distributions due to an anisotropy always point in the direction of the highest diffusivity.

Solutions which include north-south variations of the diffusivity are shown in Fig. 4. The difference between upper and lower frame side wall boundary conditions are as in Fig. 3. The source is at $y = 0.25$. No anisotropy was included for these solutions. The diffusivity varied in the north-south direction according to

$$\left.\begin{aligned} K_y &= 1 + 16\kappa_y y^2, && |y| \leqslant 0.25 \\ K_y &= 1 + \kappa_y, && |y| > 0.25 \end{aligned}\right\}. \quad (17)$$

For the above north–south variation of diffusivity α the inverse of the diffusivity length scale [Eq. (7)]

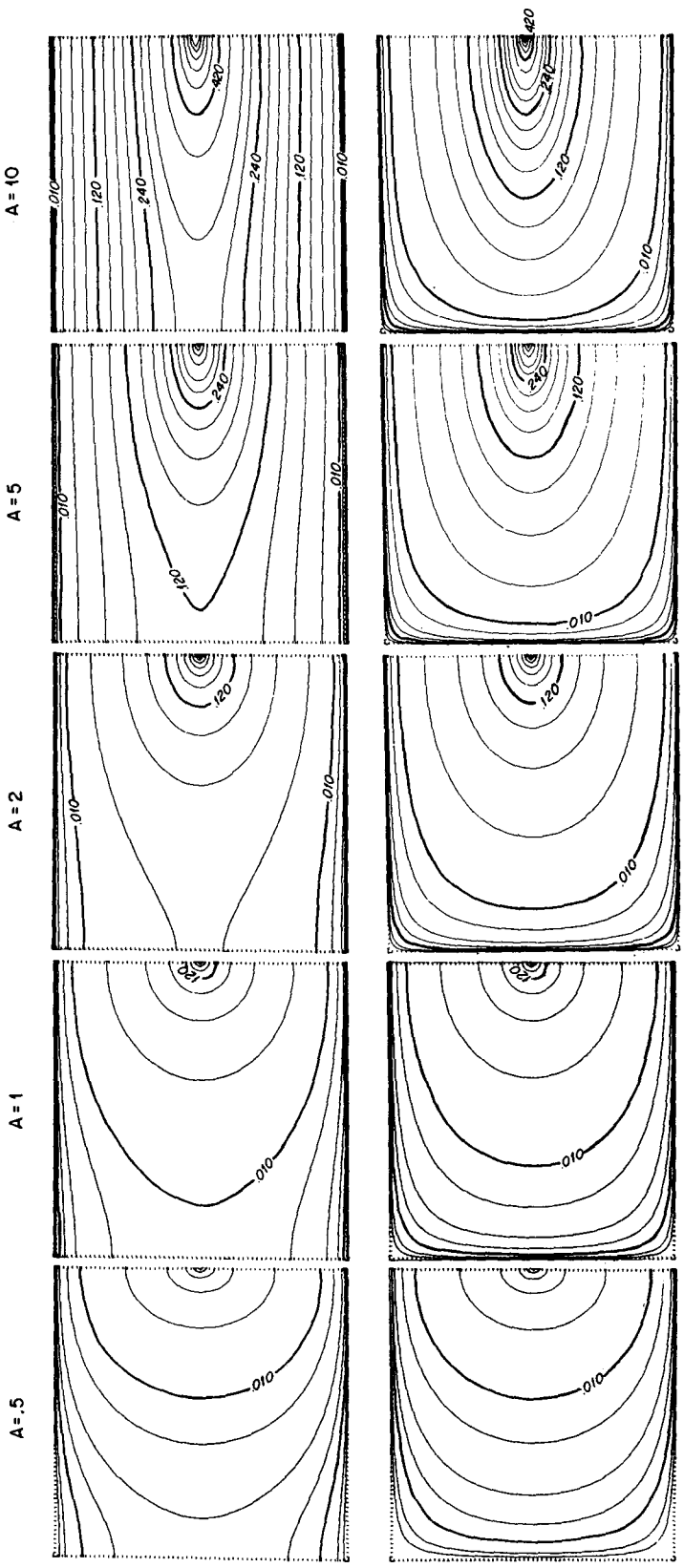

FIG. 3. Isolines of concentration showing the effects of anisotropy (A = 0.5, 1, 2, 5, 10) with a uniform diffusivity K = 1. The western boundary is insulated for the upper set of frames; for the lower set, it is a sink. For this and all succeeding contour plots, the contour levels used are: 0.0001, 0.0002, 0.0005, 0.001, 0.002, 0.005, 0.01, 0.03, 0.06, 0.09, 0.12, 0.15, 0.18, 0.21, 0.24, 0.27, 0.30, 0.36, 0.42, 0.48, 0.54, 0.60, 0.66, 0.72.

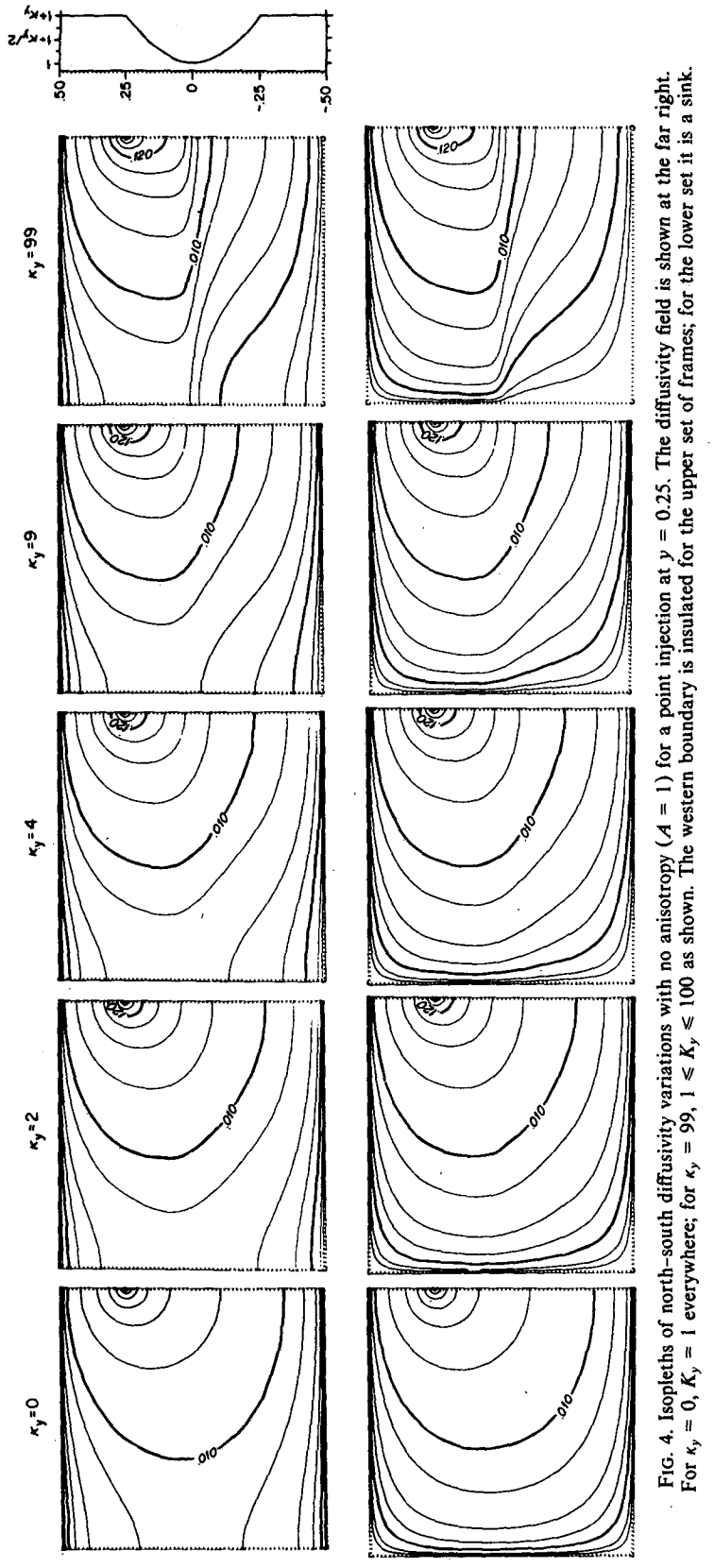

FIG. 4. Isopleths of north–south diffusivity variations with no anisotropy ($A = 1$) for a point injection at $y = 0.25$. The diffusivity field is shown at the far right. For $\kappa_y = 0$, $K_y = 1$ everywhere; for $\kappa_y = 99$, $1 \leqslant K_y \leqslant 100$ as shown. The western boundary is insulated for the upper set of frames; for the lower set it is a sink.

TABLE 1. Diffusivity K_y, and normalized diffusivity variation α, at selected positions y, along with an average Peclet number $\overline{Pe}$ for five values of K_y.

	$\kappa_y = 0$ $\overline{Pe} = 0$		$\kappa_y = 2$ $\overline{Pe} = 1.1$		$\kappa_y = 4$ $\overline{Pe} = 1.6$		$\kappa_y = 9$ $\overline{Pe} = 2.3$		$\kappa_y = 99$ $\overline{Pe} = 4.6$	
y	K_y	α	K_y	α	K_y	α	K_y	α	K_y	α
0	1	0	1	0	1	0	1	0	1	0
0.05	1	0	1.1	3.0	1.2	5.5	1.4	10.6	5.0	31.9
0.10	1	0	1.3	4.9	1.6	7.8	2.4	11.8	16.8	18.9
0.15	1	0	1.7	5.6	2.4	7.9	4.2	10.2	36.6	13.0
0.20	1	0	2.3	5.6	3.6	7.2	6.8	8.5	64.4	9.8
0.25	1	0	3.0	5.3	5.0	6.4	10.0	7.2	100.0	7.9

is given by

$$\alpha = \begin{cases} \dfrac{32\kappa_y y}{1 + 16\kappa_y y^2}, & |y| \leq 0.25 \\ 0, & |y| > 0.25 \end{cases} \quad (18)$$

For the five values of κ_y, values of K_y and α are shown in Table 1 along with the average Peclet number $\overline{Pe}$ [Eq. (13)].

As discussed in Section 2, the effect of a variable diffusivity on a steady-state concentration field is approximately logarithmic with the ratio of maximum to minimum diffusivities present in the field [Eq. (13)]. In the solutions displayed in Fig. 4, a considerable difference can be seen in the north-south distributions of concentration for the largest diffusivity variations, in comparison to the zero or low diffusivity variation solutions. For the two largest diffusivity gradients, $\kappa_y = 9$ and 99, the average Peclet numbers ($\overline{Pe} = 2.3$ and 4.6) are greater than 2, the minimum needed for an effect on the north-south property distribution [Eq. (11b)].

Solutions to the steady-state diffusion equation, with a constant diffusivity, do not depend on the actual magnitude of the diffusion coefficient [e.g., Eq. (8) with $\alpha = 0$]. In Fig. 4, the region with a spatially non-varying diffusivity at, and north of, the source at $y = 0.25$, shows only small changes in the property distributions with different magnitudes of the diffusivity. The changes are in fact due to the varying diffusivity in the central region, $|y| < 0.25$. In this central region of spatially varying diffusivity, the effect of the relatively low diffusion in the center is analogous to a divergent velocity field pointing to-

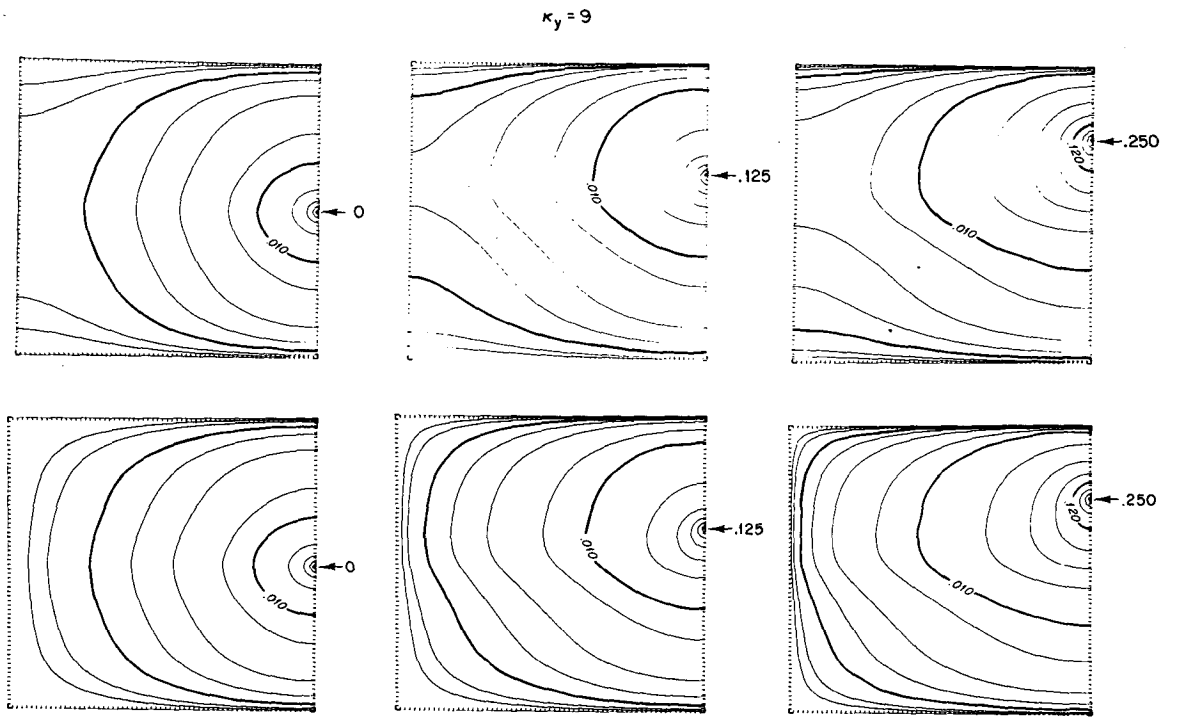

FIG. 5. The effects of varying the point of injection with the variable diffusivity field shown in Fig. 4 ($\kappa_y = 9$, $A = 1$). The western boundary is insulated for the upper set of frames; for the lower set of frames it is a sink.

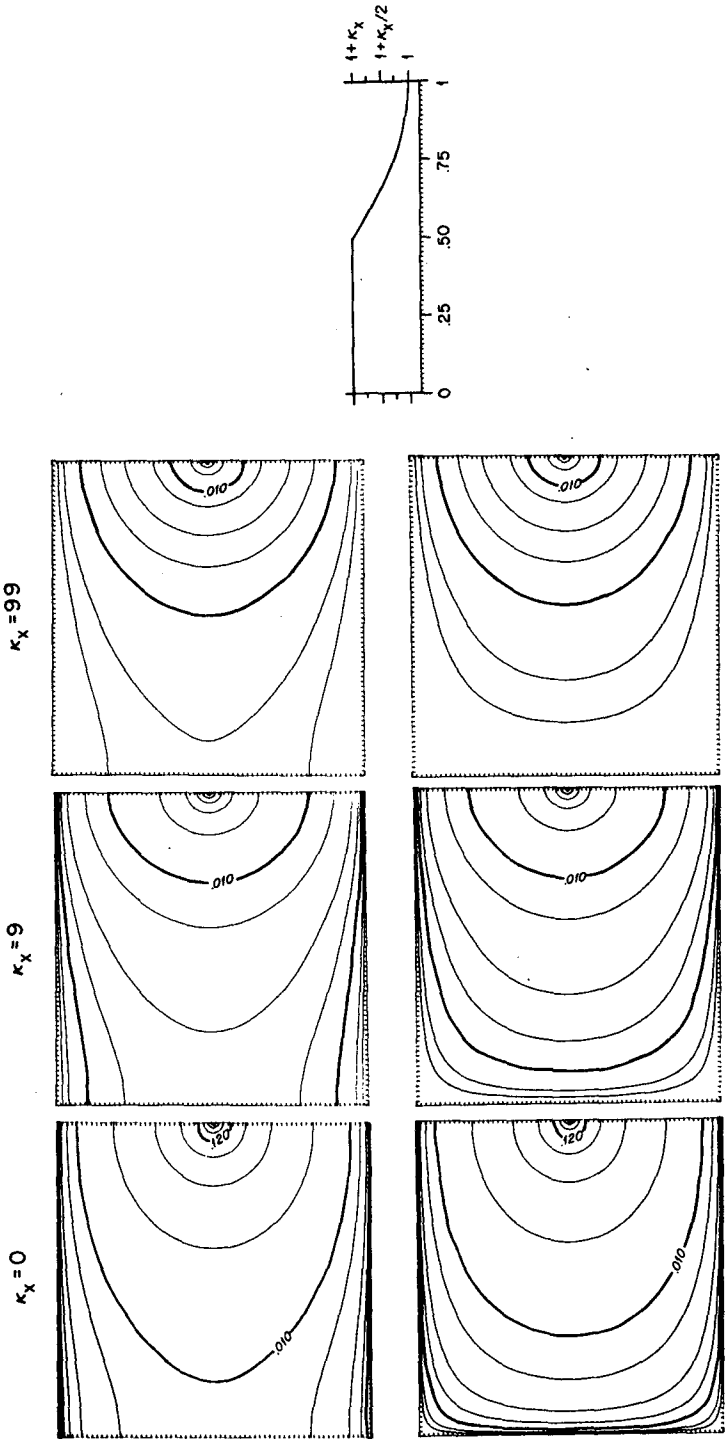

FIG. 6. East-west variations of diffusivity on a point injection at $y = 0$ ($A = 1$). The diffusivity field is shown at the far right. The western boundary is insulated for the upper set of frames; for the lower set it is a sink.

ward the low diffusivity at the center line ($y = 0$) from the relatively higher diffusivity regions to the north and south.

The effects of varying the position of the point source, with a variable diffusivity as in Fig. 4 ($\kappa_y = 9$, $A = 1$), can be seen in Fig. 5. Again, the difference in boundary conditions is as in Fig. 3. Starting from the bottom frames, a symmetric distribution is seen for a source at the center of the eastern boundary and the symmetrically varying diffusivity field. These two frames can be contrasted with the corresponding constant diffusivity field distributions shown in Fig. 3 ($A = 1$). With a varying diffusivity, a slight point or tip in the property isopleths is seen at the center line in contrast with the smooth, nearly circular isopleths in the corresponding frames of Fig. 3. As the position of the source is moved northward, more asymmetry is introduced into the resultant property distribution field. The field is also more noticeably warped by the spatially variable diffusion field.

In Fig. 6 the effects of exclusively east–west diffusivity field variations can be seen. The effects of this diffusivity distribution are similar to applying an additional velocity field from the region of high diffusivity to the region of low diffusivity, in this case analogous to adding an eastward flowing current. The source was at the center of the eastern wall, no anisotropy existed in the diffusion field, and the diffusivity varied in the east–west direction according to

$$\left.\begin{aligned} K_x &= 1 + 4\kappa_x(1-x)^2, \quad (1-x) \leqslant 0.5 \\ K_x &= 1 + \kappa_x, \qquad\qquad (1-x) > 0.5 \end{aligned}\right\}. \tag{19}$$

The three kappas shown ($\kappa_x = 0, 9, 99$) correspond to average Peclet numbers defined by Eq. (13) of $\overline{Pe} = 0$, 2.3 and 4.6, respectively. A large quantitative effect is seen for these diffusivity variations; compare, for example, the relative positions of the 0.010 isoconcentration contour. Although there is a large quantitative effect, the shape of the concentration field does not change markedly.

Two solutions for a large ($\kappa_y = 99$, $\overline{Pe} = 4.6$) one-sided north–south variation of the diffusion field are shown in Fig. 7. This particular distribution of diffusivity was chosen to simulate the oceanic case of the North Atlantic and the Mediterranean outflow. Hopefully, the eddy potential energy density map of Dantzler (1977) reproduced here in Fig. 2 represents at least qualitatively the distribution of oceanic diffusivities of the North Atlantic. The resultant property distributions with anisotropics $A = 1, 2$ are seen for an insulated western boundary and sinks to the north and south.

The property distributions due to the purely diffusive, but spatially variable, field are in fact qualitatively similar to the distributions of salinity on the density surface corresponding to the Mediterranean outflow. This distribution is shown in Fig. 1 from Reid (1979).

5. Conclusions

Tongues of various properties in the ocean have traditionally been interpreted as due to the combination of advection and diffusion. Such an interpretation will apply in areas where advection is strong relative to the gradient of the eddy diffusivity, ∇K, an advection-like term in the full advective-diffusive equation with variable diffusivity [Eq. (3)]. However, the catalog of solutions generated here suggests that the interpretation of tongues must be done with real caution when ∇K is of the same order as the velocity field. We have demonstrated how a purely diffusive field, with spatially variable or anisotropic

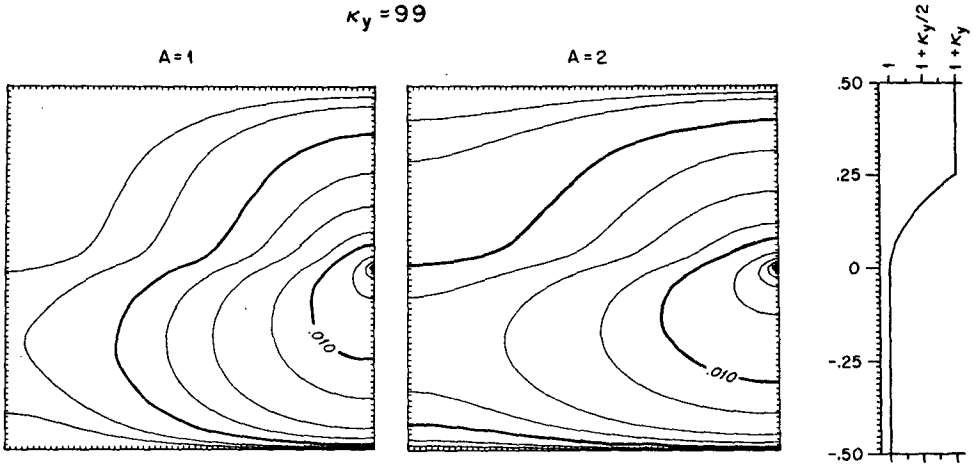

FIG. 7. Property concentrations for one-sided north-south variations in diffusivity. These results should be compared with observations and potential energy distributions shown in Figs. 1 and 2. Two anistropies ($A = 1, 2$) are shown.

diffusion, can alone generate tongue-like property distributions.

Unfortunately, an actual prescription for the oceanic diffusion field is not available and we have been forced to infer the variability from maps of eddy potential energy. These maps show variability at scales of 200 km. Using an eddy diffusivity of 10^3 m^2 s^{-1} (cf. Freeland *et al.*, 1975), a gradient diffusivity velocity of 5 mm s^{-1} is applicable even for the relatively low energy region of the Sargasso Sea studied by Freeland *et al.* At the ~1000 m level of the salinity distribution shown in Fig. 1, velocities are rarely larger than 5 mm s^{-1} based on the geopotential anomaly map of Reid (1979, Fig. 2). In the absence of more information regarding oceanic velocity and eddy fields, tongue-like property distributions need be interpreted cautiously.

Serious doubt has also recently been raised regarding the modelling of oceanic diffusion as a gradient transport process. Armi (1978) and McDowell and Rossby (1978) have shown evidence of anomalies that have moved as far as 6000 km from their presumed sources. Recently, Armi (1981) found three large lenses of anomalously high (0.8‰) salinity Mediterranean water in the Canary Basin. These lenses have diameters of 70–80 km and maximum thicknesses greater than 800 m. If they are associated with a significant transport of Mediterranean water and are not just an occasional event, then a model for tongue-like property distributions need be adopted which includes these lenses. The simplest way to treat them within the existing steady state framework would be as a distributed source, since each has a presumably different lifetime or distance travelled before breaking apart.

Acknowledgments. This research has been supported by National Science Foundation under Grants OCE 80-16125 (LA) and OCE 78-25700 (DBH); and the Office of Naval Research under Contract N00014-80-C-0440 (LA). Computing resources were provided by the National Center for Atmospheric Research, which is also funded by the National Science Foundation. This is contribution 5121 from the Woods Hole Oceanographic Institution.

REFERENCES

Armi, L., 1978: Some evidence for boundary mixing in the deep ocean. *J. Geophys. Res.*, **83,** 1971–1979.

——, 1979: Effects of variations in eddy diffusivity on property distributions in the oceans. *J. Mar. Res.*, **37,** 515–530.

——, 1981: Large lenses of highly saline Mediterranean water. *Trans. Amer. Geophys. Union,* **62,** p. 935 (Abstract 05-1-C-14).

Carslaw, H. S., and J. C. Jaeger, 1959: *Conduction of Heat in Solids,* 2nd ed. Oxford University Press, 510 pp.

Dantzler, H. L., Jr., 1977: Potential energy maxima in the tropical and subtropical North Atlantic. *J. Phys. Oceanogr.*, **7,** 512–519.

Freeland, H. P., P. Rhines and T. Rossby, 1975: Statistical observations of the trajectories of neutrally buoyant floats in the North Atlantic. *J. Mar. Res.*, **33,** 383–404.

Fuglister, F. C., 1954: Average temperature and salinity at a depth of 200 meters in the North Atlantic. *Tellus,* **6,** 46–58.

Haidvogel, D. B., and T. Zang, 1979: The accurate solution of Poisson's equation by expansion in Chebyshev polynomials. *J. Comput. Phys.*, **30,** 167–180.

Holland, W. R., 1978: The role of mesoscale eddies in the general circulation of the ocean—numerical experiments using a wind-driven quasi-geostrophic model. *J. Phys. Oceanogr.*, **8,** 363–392.

McDowell, S. E., and H. T. Rossby, 1978: Mediterranean water: an intense mesoscale eddy of the Bahamas. *Science,* **202,** 1085–1087.

Needler, G. T., and R. A. Heath, 1975: Diffusion coefficients calculated from the Mediterranean salinity anomaly in the North Atlantic Ocean. *J. Phys. Oceanogr.*, **5,** 173–182.

Price, J. F., 1981: Diffusion statistics computed from SOFAR float trajectories in the western North Atlantic. *Trans. Amer. Geophys. Union,* **62,** 937 (Abstract 05-2-B-10).

Reid, J. L., 1979: On the contribution of the Mediterranean Sea outflow to the Norwegian-Greenland Sea. *Deep-Sea Res.*, **26A,** 1199–1223.

Richardson, P. L., and K. Mooney, 1975: The Mediterranean Outflow—a simple advection-diffusion model. *J. Phys. Oceanogr.*, **5,** 476–482.

Schmitz, W. J., Jr., 1977: On the deep general circulation in the western North Atlantic. *J. Mar. Res.*, **35,** 21–28.

——, and W. R. Holland, 1982: A preliminary comparison of selected numerical eddy-resolving general circulation experiments with observations. *J. Mar. Res.*, **40,** 75–117.

Wyrtki, K., L. Magaard and J. Hager, 1976: Eddy energy in the oceans. *J. Geophys. Res.*, **81,** 2641–2646.